

COMPARISONS BETWEEN LANGMUIR PROBE MEASUREMENTS AND GLOBAL MODEL OF A CAPACITIVELY COUPLED RF ARGON DISCHARGE

F.M. Freitas^{*}; R.S. Pessoa; H.S. Maciel; G. Petraconi Filho
Instituto Tecnológico de Aeronáutica, 12.228-900, São José dos Campos, SP, Brazil

Keywords: Plasma, RIE, Global Model.

ABSTRACT

Langmuir probe measurements on radiofrequency capacitively coupled argon plasma were accomplished to obtain the plasma densities and electron temperatures. These results were compared with a global plasma model modified for this discharge geometry type. Excellent agreement between theoretical and experimental values was achieved.

1. INTRODUCTION

Planar capacitively coupled radiofrequency (RF) discharges operated at a pressure lower than 100 mtorr (13 Pa) has found widespread use on plasma processing in a diversity of fields such as surface treatment, thin-films deposition, etching, etc [1]. Currently, the study of plasma phase through diagnostic techniques (Langmuir probes, optical spectroscopy, mass spectrometry, etc.) and simulations (Monte Carlo, particle in cell, global model, etc.) is of great interest in order to understand the dependences of the plasma compositions and the electron kinetics on the external parameters [2].

In this work we measure the pressure dependence of the Langmuir probe characteristics in argon asymmetric capacitively coupled discharges and compared the results with a modified global model developed for electropositive plasma (in the sense employed by Lieberman [1]) generated in capacitively coupled geometry. This modified global model is based in global models proposed by Lieberman et al. [1], Lee et al. [3], Kimura et al. [5], and Gundmundson et al. [5], where the particle balance equations and the power balance equation are simultaneously solved by the Runge-Kutta method, in order to furnish the plasma parameters on steady-state.

2. EXPERIMENTAL

2.1. Capacitively Coupled Plasma Source and Langmuir Probe System

A schematic diagram of the experimental apparatus is shown in Figure 1. This apparatus consists of a capacitively coupled parallel plate reactor operating in RIE mode with 2 L volume and 50 mm electrode gap. The lower 13.56 MHz

RF powered electrode has 150 mm in diameter while the upper electrode is connected with the reactor walls and grounded. Prior to Ar feed the vacuum chamber is pumped down to pressure below 10^{-4} torr (10^{-4} Pa) using a combination of a roots and a mechanical pump, providing both an effective pumping speed of approximately 110 L/s. The argon gas was inserted in the chamber on a throughput range of 1–100 sccm, corresponding to a pressure range of 3–90 mtorr (0.3–12 Pa), while keeping the power P_{abs} injected into the plasma at about 50 W.

An RF compensated single Langmuir probe made of 7 mm long and 0.1 mm in diameter platinum wire is placed at the center of the reactor. The probe has a compensation circuit in order to minimize the rf oscillations in the probe circuit caused by the RF oscillations of the plasma potential. In order to obtain automated probe measurements and accuracy of the $I-V$ curves was developed a plasma diagnostic setup that is composed of a DC power supply controlled by an analog-to-digital converter device that through a PC computer automatically measures the $I-V$ plasma probe characteristic. For calculating the main plasma parameters (electron temperature, T_e , plasma density, n , and electron energy distribution function, $EEDF$), the data are processed using a routine programmed in a commercial data processing and analysis software.

2.2. Langmuir Probe I-V Characteristic Analysis Procedure

In order to obtain a better fit of experimental data with global model data we perform the following methodology of analysis for the $I-V$ probe characteristic curves measured.

A typical Langmuir probe $I-V$ characteristics for a pressure of 50 mTorr (6,7 Pa) is shown in Figure 2a. In this figure we can distinguish two different regions: the ion attraction region (ion saturation region) and the electron attraction region (transition + electron saturation regions). The extracted plasma parameters are: $n_i = 6.55 \times 10^{16} \text{ m}^{-3}$, $n_e = 3.91 \times 10^{16} \text{ m}^{-3}$ and $T_e = 1.92 \text{ eV}$. As we can see n_e tends to be less than n_i . It is known that during its operation, the current drain caused by the probe must be much smaller than the overall rate of losses of charged particles on all other mechanisms of loss, such as recombination on the walls, so as not to significantly alter the nature of the plasma. For this reason it is sometimes preferable to operate the probe in attracting ion mode, instead of the attracting electron mode, because the

^{*} fernando004@yahoo.com.br

current consumption is considerably lower (from one to two orders of magnitude) for the ion collection case. Through the probe theory is possible to determine the plasma density by the analysis of each region. However, there are several reasons for using the density obtained by the ion attraction region as the real plasma density: i) the plasma potential, V_p , where n_e is determined, is usually found from the inflection point of the curve $I-V$ or from the "knee" in which the extrapolation of the lines in regions of saturation and transition is crossing (see Figure 2b). This point is poorly defined, and n_e depends exponentially on the choice of V_p . Also, fluctuations of radiofrequency may distort this particular non-linear part of the curve; ii) the collection of large streams of electrons in the probe can in addition distort the plasma characteristics or damage the probe; iii) also, if n_i and n_e would differ by no more than 0.1%, the Poisson equation shows that d^2V/dx^2 should be the order of 200 V/cm^2 , which is impossible outside a sheath. So, unless the plasmas of low density ($n < 3 \times 10^{10} \text{ cm}^{-3}$), free of rf fields, the plasma density is better determined from the ion attraction mode, assuming quasineutrality, and any disagreement between n_i and n_e simply shows the error in measuring n_e .

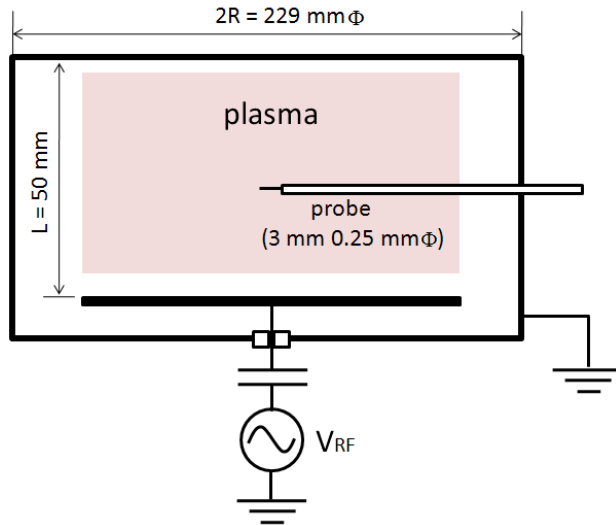


Figure 1 - Schematic diagram of experimental setup, where a frontal view of cylindrical chamber is shown. The active zone of the probe used was 3 mm long and 0.25 mm in diameter.

Thus, based in this scope the ion saturation portion of the characteristics is used to determine the ion density, n_i , and consequently the plasma density. This was determined based on the Laframboise theory [6].

The electron temperature is determined from the slope of the $\ln(I_e)-V$ curve of the probe in the region between V_f and V_p by the equation:

$$T_e = \frac{\partial V}{\partial \ln(I_e)} \quad (1)$$

where I_e is the electron current.

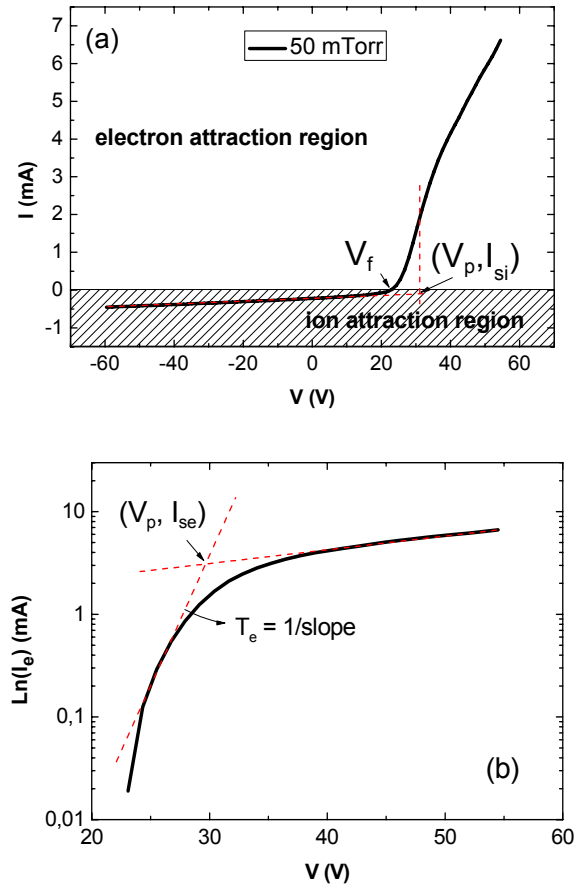


Figure 2 - (a) Langmuir probe $I-V$ characteristic, the ion saturation current is found by extrapolating the dotted line to V_p . (b) $\ln(I_e)$ versus V , the intersection of the horizontal and vertical dotted lines occurs at the coordinates (V_p, I_{se}) . The electron temperature is obtained from the slope of the linear part of the downward sloping portion of this curve.

To better explain the results it was determined the $EEDF$ for each discharge condition studied. The $EEDF$ is obtained from the second derivative of the $I-V$ curve by numerical differentiation and numerical smoothing. The measured second derivative d^2I_e/dV^2 is related to the electron energy distribution function as follows:

$$f_E(E) \Big|_{E=e(V_p-V)} = \frac{4}{A e} \left(\frac{m_e(V_p-V)}{2e} \right)^{1/2} \frac{d^2I_e(V)}{dV^2} \quad (2)$$

where e , m_e and A are the electron charge, electron mass and probe area, respectively.

3. GLOBAL MODEL

This model considers the reactions show in Table 1. The neutral density ($[Ar]$) and the charged particle density ($[Ar^+]$) was calculated in the Ar plasma maintained in a cy-

lindrical chamber of dimensions $2R$ and L , in inner diameter and length, respectively. The model considers the assumptions as follows:

- (i) The spatial profiles of n_e and the positive ion density ($[Ar^+]$) can be regarded as uniform except at the sheath.
- (ii) The *EEDF* is Maxwellian with T_e (the electron temperature in volt-equivalent units).
- (iii) The gas temperature is 300 K.

Table 1 – Reactions taken in account in the global model.

No	Reaction	Rate Coefficients	Reference
(1)	$Ar + e \rightarrow Ar^+ + 2e$	$k_{iz} = 2.3 \times 10^{-14} T_e^{0.68} e^{-15.76/T_e}$	[7]
(2)	$Ar + e \rightarrow Ar^* + e$	$k_{exc} = 2.5 \times 10^{-15} T_e^{0.74} e^{-11.56/T_e}$	[7]
(3)	$Ar + e \rightarrow Ar + e$	$k_{elas} = 2.3 \times 10^{-14} T_e^{1.61} \exp[0.06(\ln T_e)^2 - 0.12(\ln T_e)^3]$	[7]
(4)	$Ar^+ \rightarrow Ar$	$k_{Loss} = 2U_{B,Ar}(R^2 h_L + R L h_R) / R^2 L$	[3]

3.1. Particle and Power Balance

Two main sets of equations are used in this global model: particle balance for all species of interest, and power balance. As the main source of Ar on this model is the flow into the chamber, the particle balance equation for the neutral specie is given as follows:

$$\frac{d[Ar]}{dt} = (Q_f / Vol) + k_{Loss} [Ar^+] - k_{iz} [Ar] n_e - [Ar] (S_p / Vol) \quad (3)$$

where Q_f corresponds to the number density of Ar atoms flowing into the chamber per second, Vol is the chamber volume in m^3 and S_p is the pumping speed in m^3/s .

The main generation of positive ions (Ar^+) is caused by direct ionization collisions between Ar atoms and electrons, while the loss of these positive ions is due to wall neutralization. Thus, the particle balance equation for charged particles is given as follows:

$$\frac{d[Ar^+]}{dt} = k_{iz} [Ar] n_e - k_{Loss} [Ar^+] \quad (4)$$

For the power balance is assumed that all power injected into the plasma is dissipated, in part, through collision processes between electron and neutral species, while the remaining, by means of the kinetic energy of ions and electrons flowing into the walls. Taking these effects in consideration, the balance equation for energy is given as:

$$\frac{d[w_e]}{dt} = (P_{abs} / Vol) - e k_{iz} \varepsilon_c [Ar] n_e - e k_{Loss} (\varepsilon_{iw} + \varepsilon_{ew}) n_e \quad (5)$$

where:

- P_{abs} is the total power absorbed (it is assumed that the total rf power absorbed is known).
- ε_c is the collisional energy losses per electron-ion pair created and is given by,

$$\varepsilon_c = \varepsilon_{iz} + \varepsilon_{exc} \frac{k_{exc}}{k_{iz}} + (3m_e / m_{Ar}) \frac{k_{elas}}{k_{iz}} T_e \quad (6)$$

- $\varepsilon_{iw} = 2T_e$ is the electron kinetic energy lost per electron lost to the walls.
- $\varepsilon_{ew} = V_{sh} + T_e/2$ is the ion bombardment energy or the ion kinetic energy lost per ion lost to the wall.

The ion-bombarding energy is the sum of the ion energy entering the sheath and the energy gained by the ion as it traverses the sheath. The ion velocity entering the sheath is u_B , corresponding to a directed energy of $T_e/2$. The sheath edge voltage of the lower electrode [1], i.e., the energy gained by the ion to cross the sheath is given by $V_{sh} = 0.83V_1$ ($V_1 = V_{dc}$).

In equation (6), $\varepsilon_{exc} = 15.76$ eV and $\varepsilon_{iz} = 11.5$ eV are the threshold energies of the ionization and excitation [1], respectively, and k_{iz} , k_{exc} and k_{elas} are the rate constants of ionization, excitation and elastic processes, respectively (see Table 1 for rate constant expressions).

3.2. Losses to Wall

The ion flux to the walls is assumed to have rate coefficient k_{Loss} given in Table 1, where $u_B = (eT_e/m_{Ar})^{1/2}$ is the Bohm velocity, m_{Ar} is the ion mass and h_L and h_R are the edge to centre positive ion density ratios given as [1],

$$h_L = 0.86(3 + L/2\lambda)^{-1/2} \quad (7)$$

$$h_L = 0.80(4 + R/\lambda)^{-1/2} \quad (8)$$

The above equations approach the equations for an electro-positive discharge given by Godyak [8] for the regime of low pressure. Here, λ_i is the ion-neutral mean free path given by,

$$\lambda = 1/[Ar]\sigma_{Ar} \quad (9)$$

where $\sigma_{Ar} = 1 \times 10^{-18} \text{ m}^2$ is the total ion-neutral collision cross section for Ar ions [4].

3.3. Balance Equation for Charged Particles

In conjunction with the equations (3), (4) and (5) it is considered the balance equation for charged particles, considering the plasma charge neutrality, which results in,

$$n_e = [Ar^+] \quad (10)$$

The equations (3), (4), (5) and (10) are solved as time evolutions of neutral and charged particles densities and electrons energy density by the Runge-Kutta method. The correspondent solutions for the steady-state were considered to be achieved from the time when no more significant variations were present in the densities data.

4. RESULTS AND DISCUSSION

Figures 3 and 4 illustrate the plasma density and electron temperature of electrons as a function of gas pressure, respectively. In these figures is possible to establish a comparison between the experimental data and the calculated results obtained by the use of the global model simulation. Although the excellent consistence of the simulated results on the plasma densities measured, for electron temperature (Figure 4), they show an augmenting divergence from the measured values at lower pressures. This result reflects the deviation from the Maxwellian distribution that occurs at pressures lower than 20 mTorr as can be observed in Figure 5. In fact, the global model considers a Maxwellian velocity distribution throughout the pressure range, what causes it inaccuracy at low pressure regime [1]. Nonetheless, the physical and chemical processes in the Ar discharge can be explained using the model.

The increase in the gas pressure (or throughput) results in the increase of the gas ionization. It enhancement can follow different mechanisms. Which will be dominant depends on the nature of the gas and on the pressure range where the discharge operates. The first obvious channel is simply the increase of ionizing collision due to the presence of more argons atoms available to be ionized. Other path that increases in importance as pressure rises is the participation of Ar metastables in the ionization balance (through a two-step ionization mechanism). Although the importance of this latter mechanism, there is a lack of basic information of this

process, as cross-section, collision frequency, etc [9]. This makes the analysis of its contribution a difficult task. Another mechanism not investigated on this article is the decreasing in the losses to the walls. The Global Model should be improved to investigate this phenomenon.

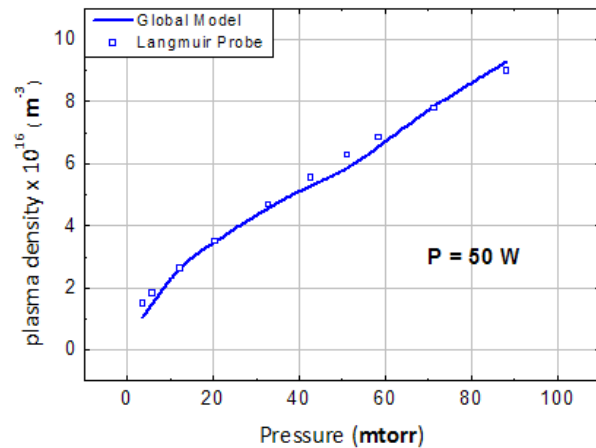


Figure 3 - Comparison of experimental and theoretical Argon throughput on electron density.

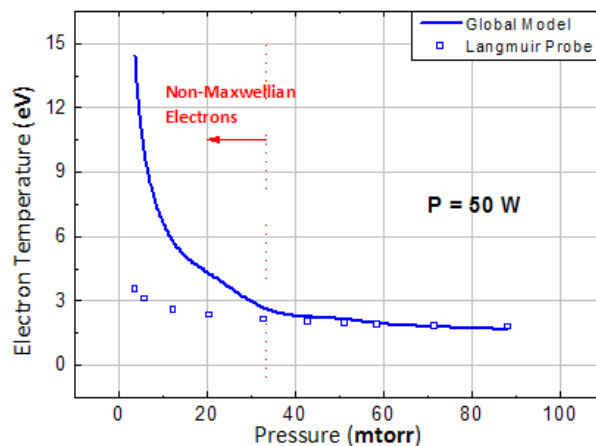


Figure 4 - Comparison of experimental and theoretical Argon throughput on electron temperature.

Two-temperature electron density distributions were already reported in literature [10]. This phenomenon has been explained as a transition from stochastically to ohmically dominated electron heating [1]. In the stochastic heating, the electron density distribution is not Maxwellian, but is a time-varying function with a time-varying electron density at the electron sheath edge [1]. In the ohmic heating the time-average power per unit area deposited in the bulk plasma is due to collisional momentum transfer between the oscillating electrons and the neutrals.

The small differences between the calculated results and the measured ones can be accounted for many factors. First, imprecision inherent to the electrostatic probe technique add, to a certain amount, errors to the measured results. Another factor that deserves further comments is the fact that metastables were not considered on this model. Their presence

can presents another process of ionization and, consequently, promoting a better adjustment of plasma density, because in argon plasmas the presence of metastables is high and has a great influence on the kinetics of the particles [7]. At least, the asymmetry of the discharge was only considered on the sheath voltage calculation, but it should be take into account on the ion loss constant, ion Bohm velocity and effective area calculations too.

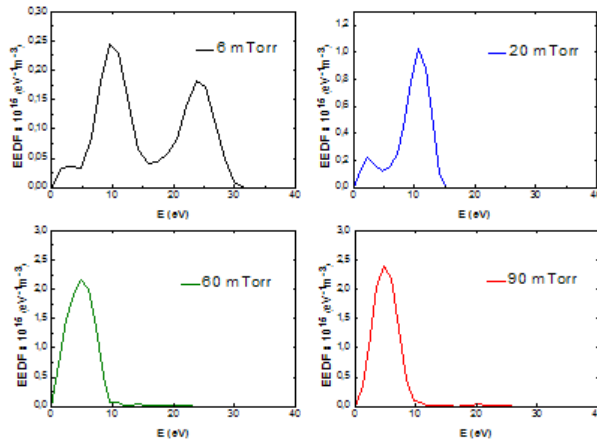


Figure 5 - The measured EEDFs at various gas pressures: (a) 6 mtorr, (b) 20 mtorr, (c) 60 mtorr, and (d) 90 mtorr.

5. CONCLUSION

A global model for argon discharges has been developed. The model consists of rate equations for neutrals and charged particles, and an energy balance equation for electrons. The model prediction approximates the laboratorial results.

A further improvement on simulated results can be achieved by additional species on the global model as meta-stables, and excited atoms and ions. This extension of the plasma model presented herein will be performed in future works.

ACKNOWLEDGEMENTS

The financial support of CNPq – Programa Nacional de Microeletrônica is strongly acknowledged.

REFERENCES

1. LIEBERMAN, M.A.; LICHTENBERG, A.J., *Principles of Plasma Discharge and Material Processing*, Wiley, New York, 1994.
2. LEE C.; LIEBERMAN M.A., *J. Vac. Sci. Technol. A* 13 (1995) 368-380.
3. YAN, M.; BOGAERTS, A.; GOEDHEER, W.J.; GIJBELS, R., *Plasma Sources Sci. Technol.* 9 (2000) 583-591.
4. KIMURA, T.; OHE, K., *Plasma Sources Sci. Technol.* 8 (1999) 553-560.
5. GUDMUNDSSON, J.T.; KIMURA, T.; LIEBERMAN, M.A., *Plasma Sources Sci. Technol.*, 8 (1998) 22-30.
6. CHEN, F.F., *Phys. of Plasmas*, 8 (2001) 3029-3041.
7. LEE M.; JANG S.; CHUNGA C., *Phys. of Plasmas* 13 (2006) 053502.
8. GODYAK, V.A., *Soviet Radio Frequency Discharge Research*, Delphic Associates, Falls Church, VA, 1986.
9. CHAPMAN, B., *Glow Discharge Processes*, Wiley, New York, 1980.
10. GODYAK, V.A.; PIEJAK, R. B., *Phys. Rev. Lett.*, 65 (1990) 996-999.